

Cite this: DOI: 10.1039/c0xx00000x

www.rsc.org/xxxxxx

ARTICLE TYPE

## CaH<sub>2</sub>-assisted low temperature synthesis of metallic magnetic nanoparticle-loaded multiwalled carbon nanotubes

Liis Seinberg<sup>a</sup>, Shinpei Yamamoto<sup>\*b</sup>, Masahiko Tsujimoto<sup>b</sup>, Yoji Kobayashi<sup>a</sup>, Mikio Takano<sup>b</sup> and Hiroshi Kageyama<sup>a,b,c</sup>

<sup>5</sup> Received (in XXX, XXX) Xth XXXXXXXXXX 20XX, Accepted Xth XXXXXXXXXX 20XX

DOI: 10.1039/b000000x

We studied synthesis of Ni or Fe nanoparticle-loaded multiwalled carbon nanotubes (MWCNTs) by pyrolyzing metal organic salts with CaH<sub>2</sub>, a very strong reductant. The use of CaH<sub>2</sub> lowered formation temperature of MWCNTs down to 400 °C without using toxic halogen-containing precursors and assistance of plasma.

Carbon nanotubes (CNTs) have attracted much attention since the report by Iijima due to their special physical and chemical properties.<sup>1,2</sup> A number of methods, *e.g.*, arc discharge, electrolysis, laser ablation, sonochemical and hydrothermal methods, and chemical vapour deposition (CVD) have been developed for preparation of CNTs.<sup>3</sup> Nowadays, the CVD methods are the most widely used but reaction temperatures higher than 600 °C are typically necessary.<sup>4</sup> Additional drawbacks of the CVD methods are the necessity of complex equipment, and an external carbon source or catalyst feedstock during the synthesis.<sup>3</sup>

Pyrolysis of metal organic salt to form CNTs is one variant of the CVD method. In this method, metallic nanoparticles (NPs) which act as catalysts are formed *in-situ* via reduction of metal ions by the decomposed organic ligands upon heating.<sup>5</sup> MWCNTs loaded with metallic Ni and Fe NP can be prepared by pyrolyzing nickel stearate or ferrocene, respectively, under a flow of acetylene at 800 - 1100 °C.<sup>5</sup> This method is quite simple and considered to be suitable for mass production, thus directing our main focus on this method. However, this method requires high reaction temperatures partly because the reducing agents necessary to form metallic NPs, *i.e.*, decomposed organic ligands, have poor reducing ability at low temperatures. Thus, the addition of strong reducing agent which enables the formation of metallic NP catalysts at lower temperatures is expected to accomplish CNT formation at lower temperatures.

Several reports in solid state chemistry have shown that CaH<sub>2</sub> is a fairly strong reductant for metal oxides at low temperatures (< 300 °C).<sup>6,7</sup> Our recent work demonstrated this method can also be applied to reduction of metal organic salts.<sup>8</sup> Metallic Fe and Ni NPs, which are known to be efficient catalysts for MWCNT formation, can be prepared at temperatures as low as 140 °C simply by reducing the

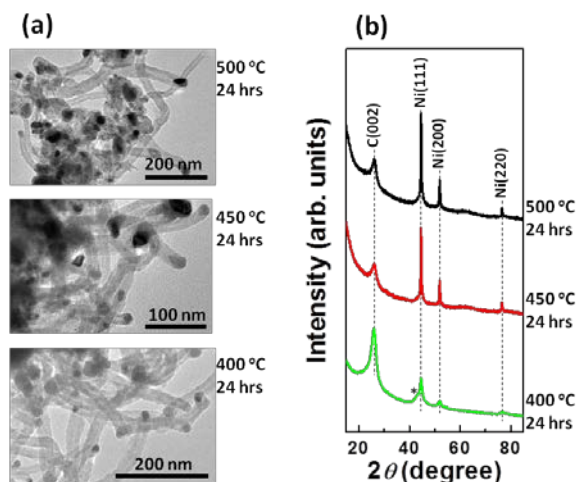


**Fig. 1** (a) TEM images and (b) XRD patterns of the samples prepared with Ni(SA)<sub>2</sub> at 500, 450 and 400 °C for 24 hrs. Asterisk (\*) represents (004) peak of graphite.

corresponding metal organic salts with CaH<sub>2</sub>.<sup>8</sup> Here, we report a low temperature synthesis of Ni or Fe NP-loaded multiwalled CNTs (MWCNTs) by pyrolyzing metal organic salts with CaH<sub>2</sub>. Such CNTs decorated with magnetic NPs have found advanced applications especially in the field of biomedicine and biotechnology due to the multiple functionalities.<sup>9</sup> The most representative feature of our method is the low reaction temperature (400 °C); this is much lower than those of the pyrolysis method (> 800 °C).<sup>5</sup> and the typical CVD methods (> 600 °C).<sup>4</sup> A facile one-step synthetic procedure, no external carbon source, and no catalyst feedstock during the synthesis are also noteworthy.

Mixtures of CaH<sub>2</sub> and nickel(II) stearate (Ni(SA)<sub>2</sub>) or iron(III) stearate (Fe(SA)<sub>3</sub>) were sealed in a pyrex tube under inert atmosphere and heat-treated at 300, 350, 400, 450 and 500 °C. After the reaction, the samples were washed to remove by-products and unreacted CaH<sub>2</sub>. Details of the synthesis are described in Electronic Supplementary Information (ESI).

Fig. 1a shows transmission electron microscopic (TEM) images of the samples prepared with Ni(SA)<sub>2</sub> at 400, 450 and 500 °C for 24 hrs. All sample showed formation of MWCNTs.

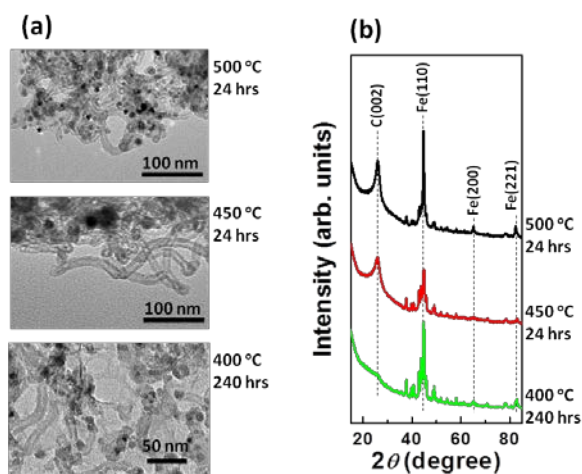


**Fig. 2** (a) TEM images and (b) XRD patterns of the samples prepared with  $\text{Fe}(\text{SA})_3$  at 500 and 450 °C for 24 hrs and 400 °C for 240 hrs. The other non-indexed small peaks are from  $\text{Fe}_3\text{C}$  (see Figure S2 in ESI).

**Table 1. Properties of the as-prepared samples.**

	Ni(SA) <sub>2</sub>			Fe(SA) <sub>3</sub>		
	500	450	400	500	450	400
$T_r$ <sup>a)</sup> (°C)	500	450	400	500	450	400
$D_{\text{MWCNT}}$ <sup>b)</sup> (nm)	20 ± 4	25 ± 5	31 ± 9	13 ± 2	17 ± 4	- <sup>b)</sup>
$D_{\text{NP}}$ <sup>b)</sup> (nm)	16 ± 7	20 ± 6	26 ± 10	7 ± 3	12 ± 3	14 ± 4
$L$ <sup>b)</sup> (μm)	2.4 ± 0.8	2.0 ± 0.7	1.5 ± 0.4	0.19 ± 0.07	0.23 ± 0.08	- <sup>b)</sup>
$I_D/I_G$ <sup>c)</sup>	1.1	0.9	1.4	1.5	1.5	1.4
$\sigma$ <sup>d)</sup>	0.19	0.24	0.09	0.20	0.18	0.38
Yield <sup>e)</sup> (%)	33	27	25	26	19	14

- a) Reacted for 24 hrs except for the case of 400 °C with  $\text{Fe}(\text{SA})_3$  (240 hrs).  
 b) Shown as mean ± standard deviation estimated on the average of > 100 samples in the TEM images.  
 c) Relative intensity ratio of the D and G band peaks in the Raman spectra.  
 d) Determined by thermogravimetric analyses (see Figure S11 in ESI).  
 e) Relative to the amount of the starting salt ( $\text{Ni}(\text{SA})_2$  or  $\text{Fe}(\text{SA})_3$ ).  
 f) Unable to estimate statistical values due to less MWCNTs observed.

Fig. 1b shows powder X-ray diffraction (XRD) patterns for the same samples. They show three relatively sharp diffraction peaks assigned to {111}, {200} and {220} planes of face-centered cubic (fcc) structure of metallic Ni, in addition to a broad peak characteristic of the {002} graphitic carbon plane<sup>5</sup> at  $20^\circ < 2\theta < 30^\circ$ . Lower temperature reactions (< 400 °C) can yield metallic Ni NP but no MWCNTs (see Figure S1 in ESI).

Fig. 2a shows TEM images of the samples prepared with  $\text{Fe}(\text{SA})_3$  at 500 and 450 °C for 24 hrs and 400 °C for 240 hrs. Formation of MWCNT was clearly observed. Fig. 2b shows XRD patterns for the same samples. There are three relatively sharp peaks, which could be assigned to {110}, {200} and {221} planes of body-centered cubic (bcc) structure of metallic Fe. A broad peak characteristic of {002} graphitic carbon plane again appears at  $20^\circ < 2\theta < 30^\circ$ . The other small peaks are from cementite,  $\text{Fe}_3\text{C}$  (see Figure S2 in ESI). Reactions under milder conditions did not yield MWCNTs (see Figure S3 in ESI). It should be noted that the reactions at 400 °C can yield MWCNTs but the amount was very small. Fe NPs without MWCNTs are mainly observed.

Both Figs. 1a and 2a reveal that one metal NP is located near the tip of the MWCNT. Obviously, the MWCNT formation takes place by the tip growth mechanism, where the formation of metal NP is followed by carbon atoms deposition, resulting in MWCNTs growth.<sup>4</sup> This is consistent with the

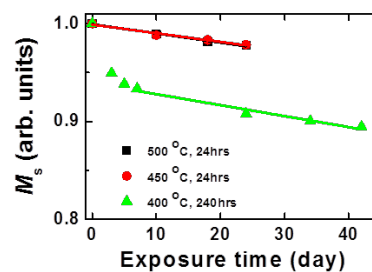


**Fig. 3** Time evolution of  $M_s$  of the Fe NP-loaded MWCNTs. The as-prepared samples have  $M_s$ s of 22, 21 and 42 emu/g for  $T_r = 500$ , 450 and 400 °C, respectively. The linear lines are the least squares fittings used to estimate daily decrease in  $M_s(d)$ . For values of  $d$ , see Table S1 in ESI.

previous results obtained at higher temperatures.<sup>5,10</sup> Some structural parameters are shown in Table 1. Outer diameter of the MWCNTs ( $D_{\text{MWCNT}}$ ) can be controlled by reaction temperature ( $T_r$ ): higher  $T_r$  gives smaller  $D_{\text{MWCNT}}$ . Size of catalyst NPs is known to have strong influences on  $D_{\text{MWCNT}}$ .<sup>11</sup> Diameter of the metallic NPs ( $D_{\text{NP}}$ ) actually decreases with increasing  $T_r$ . This unusual temperature dependence of  $D_{\text{NP}}$  was also observed in the previous work and might be explained by more nucleation sites for NP growth at higher temperatures.<sup>8</sup> Table 1 reveals that macroscopic structures such as  $D_{\text{MWCNT}}$ ,  $D_{\text{NP}}$  and length of MWCNTs ( $L$ ) depend on  $T_r$ . Microscopic structures, on the other hand, are less dependent on  $T_r$ , as revealed by relative intensity ratio of the D and G band peaks ( $I_D/I_G$ ) in the Raman spectra (Table 1 and Figure S4 in ESI for the spectra) and high magnification TEM images (Figures S5-10 in ESI). Wall number varies depending on positions along CNT but was < 20 independent of the samples. It's worth noting that Fe NP-loaded MWCNTs have more defects (kinks) than Ni NP-loaded ones.

For practical applications, stability under air is particularly important. Fig. 3 shows time evolution of saturation magnetization ( $M_s$ ) at room temperature of the Fe NP-loaded MWCNTs upon exposure to air up to 40 days. Here,  $M_s$  is defined as magnetization at an external magnetic field of 5 T normalized by the net sample weight. The as-prepared samples have  $M_s$  of ~ 20 ( $T_r = 500$  and 450 °C) and 42 emu/g ( $T_r = 400$  °C), which in turn, ~ 110 emu/g-Fe independent of  $T_r$  (see Table 1 for the weight fraction of magnetic element ( $\sigma$ ) in the samples). Several factors are responsible for the smaller values than the ideal one (218 emu/g- $\text{Fe}^{12}$ ); presence of  $\text{Fe}_3\text{C}$  with a smaller saturation magnetization (~ 140 emu/g<sup>13</sup>), oxidation during the washing under air and predominance of non-magnetic surface layer due to the small particle size.<sup>14</sup> The samples prepared at higher  $T_r$ s have fairly good stability, *i.e.*, daily decrease in  $M_s(d)$  of 0.1 %. The sample prepared at 400 °C, on the other hand, showed ~ 9 % decrease in  $M_s$  during the initial 7 days probably due to rapid oxidation of the Fe NPs without MWCNTs. Quantitative estimation of stability of the Fe NP-loaded MWCNTs formed at 400 °C was rather difficult because of the minor fraction in the sample. The other magnetic properties are given in ESI (Figure S12 and Table S1).

The present data clearly demonstrate that the use of  $\text{CaH}_2$

enables formation of well crystallized Ni and Fe NP-loaded MWCNTs even at 400 °C. This is markedly low compared to those by the pyrolysis method (800 – 1000 °C) and the typical CVD methods (600 – 1000 °C). Then, how can such low reaction temperatures be realized? Previous works help us to find the keys for lower temperature formation of CNTs. MWCNT synthesis less than 200 °C was reported by using toxic halogen-containing precursors having weaker carbon-halogen bonds.<sup>15</sup> Assistance of plasma which facilitates decomposition of carbon feedstocks can lower formation temperature of MWCNT and single walled carbon nanotube (SWCNT) down to 450 and 400 °C, respectively.<sup>16</sup> Although normal CVD synthesis of SWCNT at 350 °C was reported,<sup>17</sup> most of the low temperature synthesis works strongly suggest importance of lowering decomposition temperature of carbon feedstocks.<sup>18</sup>

An important role of CaH<sub>2</sub> is formation of Ni or Fe NPs which act as catalyst at lower temperatures, as described. We consider in addition that CaH<sub>2</sub> has another important role; facilitating decomposition of organic ligands via reactions including removal of oxygen atoms (see Figure S13 in ESI for details). This is because XRD measurement of the crude reaction mixture revealed formation of CaO (see Figure S14 in ESI) and the fact that only the organic ligand (stearate) has oxygen atoms. This idea is further supported by the fact that the reaction with ferrocene, an iron organic salt with no oxygen atoms, formed no MWCNTs even at 500 °C (see Figure S15 in ESI). These dual roles of CaH<sub>2</sub> are considered to be responsible for such low temperature formation of the MWCNTs (see also Figure S16 in ESI for details).

In conclusion, we have successfully synthesized MWCNTs loaded with Ni or Fe NP by pyrolyzing metal organic salt with CaH<sub>2</sub>. The use of CaH<sub>2</sub> enables formation of MWCNTs at 400 °C without using toxic halogen-containing precursors and assistance of plasma. This is about half of the lowest reported temperature in the pyrolysis method and among the lowest formation temperature by the typical CVD methods. The dual roles of CaH<sub>2</sub> are considered to be responsible for such extraordinary low formation temperature; formation of metal NPs which act as catalyst at lower temperatures and enhancement of decomposition of the carbon feedstocks. This work clearly demonstrates that CaH<sub>2</sub> opens a way to low temperature synthesis of MWCNTs loaded with a variety of metal NP able to catalyze CNT growth, *e.g.*, Fe, Co, Ni, Cu, Pd, Ag, Pt and Au.<sup>4</sup>

This work was supported in part by CREST, the Global COE Program “Integrated Material Science” (No. B-024) from MEXT of Japan, Murata Science Foundation and the Japan-U.S. Cooperative Science Program (No. 14508500001) from JSPS and NSF.

## Notes and references

<sup>a</sup> Department of Energy and Hydrocarbon Chemistry, Graduate School of Engineering, Kyoto University, Nishikyo-ku, Kyoto, 615-8510, Japan.

<sup>b</sup> Institute for Integrated Cell-Material Sciences, Kyoto University, Yoshida-Ushinomiya-cho, Sakyo-ku, Kyoto, 606-8501, Japan. FAX: +81-

75-753-9820; TEL: + 81-75-753-9861; E-mail: [yamamoto@icems.kyoto-u.ac.jp](mailto:yamamoto@icems.kyoto-u.ac.jp)

<sup>c</sup> CREST, Japan Science and Technology Agency (JST)

<sup>†</sup> Electronic Supplementary Information (ESI) available: Details of the synthesis and characterization methods, and complementary data (Figures S1-S18 and Tables S1 and S2). See DOI: 10.1039/b000000x

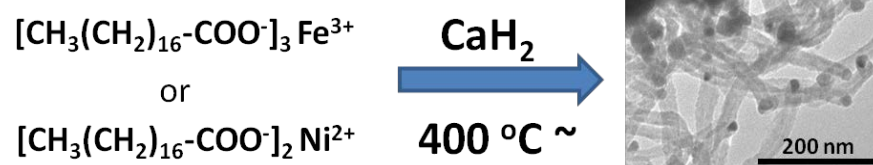
- 1 S. Iijima *Nature*, 1991, **354**, 56.
- 2 J. M. Schnorr and T. M. Swager, *Chem. Mater.* 2011, **23**, 646; Z. Xiong, Y. S. Yun and H.-J. Jin, *Materials*, 2013, **6**, 1138; K. V. Wong and B. Bachelier, *J. Energy Resour. Technol.* 2014, **136**, 021601-1; S. Vardharajula, S. Z. Ali, P. M. Tiwari, E. Eroglu, K. Vig, V. A. Dennis and S. R. Singh, *Int. J. Nanomedicine*, 2012, **7**, 5361; S. Park, M. Vosguerichian and Z. Bao, *Nanoscale*, 2013, **5**, 1727; Q. Zhang, J.-Q. Huang, W.-Z. Qian, Y.-Y. Zhang and F. Wei, *Small*, 2013, **9**, 1237; M. F. L. D. Volder, S. H. Tawfick, R. H. Baughman and A. J. Hart, *Science*, 2013, **339**, 535.
- 3 J. Parasek, J. Drbohlavova, J. Chomoucka, J. Hubalek, O. Jasek, V. Adam and R. Kizek, *J. Mater. Chem.*, 2011, **21**, 15872; A. Szabó, C. Perri, A. Csató, G. Giordano, DVuono, J. B. Nagy, *Materials*, 2010, **3**, 3092.
- 4 M. Kumar and Y. Ando, *J. Nanosci. Nanotechnol.*, 2010, **10**, 3739; D. Varshney, B. R. Weiner and G. Morell, *Carbon*, 2010, **48**, 3353; J. Kang, J. Li, X. Du, C. Shi, N. Zhao and P. Nash, *Mat. Sci. Eng. A*, 2008, **475**, 136.
- 5 F. Geng, D. Jefferson and B. F. G. Johnson, *J. Mater. Chem* 2005, **15**, 844; B. C. Satishkumar, A. Govindaraj, P.V. Vanitha, A. K. Raychaudhuri and C.N.R. Rao, *Chem. Phys. Lett.* 2002, **362**, 301; F. Geng, D. A. Jefferson and B. F. G. Johnson, *Chem. Commun.*, 2004, 2442.
- 6 M. A. Hayward, E. J. Cussen, J. B. Claridge, M. Bieringer, M. J. Rosseinsky, C. J. Kiely, S. J. Blundell, I. M. Marshall and F. L. Pratt, *Science*, 2002, **295**, 1882; Y. Tsujimoto, C. Tassel, N. Hayashi, T. Watanabe, H. Kageyama, K. Yoshimura, M. Takano, M. Ceretti, C. Ritter and W. Paulus, *Nature*, 2007, **450**, 1062; L. Seinberg, T. Yamamoto, C. Tassel, Y. Kobayashi, N. Hayashi, A. Kitada, Y. Sumida, T. Watanabe, M. Nishi, K. Ohoyama, K. Yoshimura, M. Takano, W. Paulus and H. Kageyama, *Inorg. Chem.*, 2011, **50**, 3988;
- 7 S. Yamamoto, R. Gallage, Y. Tamada, K. Kohara, Y. Kusano, T. Sasano, K. Ohno, Y. Tsujii, H. Kageyama, T. Ono and M. Takano, *Chem. Mater.*, 2011, **23**, 1564; K. Kohara, S. Yamamoto, L. Seinberg, T. Murakami, M. Tsujimoto, T. Ogawa, H. Kurata, H. Kageyama and M. Takano *Chem. Commun.*, 2013, **49**, 2563.
- 8 L. Seinberg, S. Yamamoto, R. Gallage, M. Tsujimoto, Y. Kobayashi, S. Isoda, M. Takano and H. Kageyama, *Chem. Commun.*, 2012, **48**, 8237.
- 9 A. Masotti and A. Caporali, *Int. J. Mol. Sci.*, 2013, **14**, 24619.
- 10 *Inorganic Nanoparticles Synthesis Applications and Perspectives*, ed. C. Altavilla and E. Ciliberto, CRC Press, 2010.
- 11 C. L. Cheung, A. Kurtz, H. Park and C. M. Leiber, *J. Phys. Chem. B*, 2002, **106**, 2429.
- 12 D. L. Huber, *Small* 2010, **1**, 482.
- 13 L. J. E. Hofer and E. M. Cohn, *J. Am. Chem. Soc.*, 1959, **81**, 1576.
- 14 D. H. Han and J. P. Wang and H. L. Luo, *J. Magn. Magn. Mater.*, 1994, **136**, 176.
- 15 X. Wang, J. Lu, Y. Xie, G. Du, Q. Guo and S. Zhang, *J. Phys. Chem. B*, 2002, **106**, 933; J. K. Vohs, J. J. Brege, J. E. Raymond, A. E. Brown, G. L. Williams and B. D. Fahlman, *J. Am. Chem. Soc.*, 2004, **126**, 9936.
- 16 E. J. Bae, Y.-S. Min, D. K. Kang, J.-H. Ko and W. Park, *Chem. Mater.*, 2005, **17**, 5141; J. I. B. Wilson, N. Scheerbaum, S. Karim, N. Polwart, P. John, Y. Fan and A. G. Fitzgerald, *Diam. Relat. Mater.*, 2002, **11**, 918.
- 17 M. Cantoro, S. Hofmann, S. Pisana, V. Scardaci, A. Parvez, C. Ducati, A. C. Ferrari, A. M. Blackburn, K.-Y. Wang and J. Robertson, *Nano Lett.*, 2006, **6**, 1107.
- 18 E. Mora, J. M. Pigos, F. Ding, B. I. Yakobson and A. R. Harutyunyan, *J. Am. Chem. Soc.*, 2008, **130**, 11840.

Cite this: DOI: 10.1039/c0xx00000x

[www.rsc.org/xxxxxxx](http://www.rsc.org/xxxxxxx)

ARTICLE TYPE

## Graphical and Textual Abstract for the Table of Content



Ni or Fe nanoparticle-loaded multiwalled carbon nanotubes can be prepared even at 400 °C by simply heating metal organic salts with CaH<sub>2</sub>.